OPEN

Experimental & Molecular Medicine (2013) 45, e29; doi:10.1038/emm.2013.56

www.nature.com/emm

ORIGINAL ARTICLE

Synapsin-1 and tau reciprocal *O*-GlcNAcylation and phosphorylation sites in mouse brain synaptosomes

Min Jueng Kang[1], Chaeyoung Kim[2], Hyobin Jeong[3], Byoung-Kyu Cho[1], Ae Lan Ryou[1], Daehee Hwang[3], Inhee Mook-Jung[2] and Eugene C Yi[1]

***O*-linked *N*-acetylglucosamine (*O*-GlcNAc) represents a key regulatory post-translational modification (PTM) that is reversible and often reciprocal with phosphorylation of serine and threonine at the same or nearby residues. Although recent technical advances in *O*-GlcNAc site-mapping methods combined with mass spectrometry (MS) techniques have facilitated study of the fundamental roles of *O*-GlcNAcylation in cellular processes, an efficient technique for examining the dynamic, reciprocal relationships between *O*-GlcNAcylation and phosphorylation is needed to provide greater insights into the regulatory functions of *O*-GlcNAcylation. Here, we describe a strategy for selectively identifying both *O*-GlcNAc- and phospho-modified sites. This strategy involves metal affinity separation of *O*-GlcNAcylated and phosphorylated peptides, β-elimination of *O*-GlcNAcyl or phosphoryl functional groups from the separated peptides followed by dithiothreitol (DTT) conjugation (BEMAD), affinity purification of DTT-conjugated peptides using thiol affinity chromatography, and identification of formerly *O*-GlcNAcylated or phosphorylated peptides by MS. The combined metal affinity separation and BEMAD approach allows selective enrichment of *O*-GlcNAcylated peptides over phosphorylated counterparts. Using this approach with mouse brain synaptosomes, we identified the serine residue at 605 of the synapsin-1 peptide, ^{603}QASQAGPGPR^{612}, and the serine residue at 692 of the tau peptide, ^{688}SPVVSGDTSPR^{698}, which were found to be potential reciprocal *O*-GlcNAcylation and phosphorylation sites. These results demonstrate that our strategy enables mapping of the reciprocal site occupancy of *O*-GlcNAcylation and phosphorylation of proteins, which permits the assessment of cross-talk between these two PTMs and their regulatory roles.**
Experimental & Molecular Medicine (2013) **45,** e29; doi:10.1038/emm.2013.56; published online 28 June 2013

Keywords: BEMAD; *O*-GlcNAcylation; phosphorylation; synapsin-1; synaptosome; tau

INTRODUCTION

The addition of an *O*-linked *N*-acetylglucosamine (*O*-GlcNAc) is a dynamic post-translational modification (PTM) of serine and threonine residues of nuclear and cytoplasmic proteins that is recognized as a key regulatory process involved in nuclear transport, transcription and translation, signal transduction, cytoskeletal reorganization, proteasomal degradation and apoptosis.[1] The regulatory *O*-GlcNAcylation process, which is catalyzed by coordinated actions of *O*-GlcNAc transferase and *O*-GlcNAc amidase, is reversible and often reciprocal with serine and threonine phosphorylation at the same or nearby residues.[2] The dynamic interplay between *O*-GlcNAcylation and phosphorylation and their regulatory mechanisms in signaling, transcription and chronic disease have been extensively reviewed by Hart *et al.*[3] More recently, Mishra *et al.* hypothesized that phosphorylation could be a prerequisite for *O*-GlcNAcylation and that tyrosine phosphorylation has a role in the interplay between serine/threonine *O*-GlcNAcylation and phosphorylation.[4]

Various enrichment strategies for isolating *O*-GlcNAcylated peptides coupled with mass spectrometry (MS) techniques have been used to map *O*-GlcNAc sites. These methods include GlcNAc-binding lectin wheat germ agglutinin (WGA) affinity purification,[5,6] enzymatic labeling of protein *O*-GlcNAc with *N*-azidoacetylgalatosamine, chemical attachment of a biotin tag followed by affinity purification and ETD MS to identify *O*-GlcNAc sites,[7] and selective enrichment of *O*-GlcNAcylated peptides using BEMAD or biotin

[1]WCU Department of Molecular Medicine and Biopharmaceutical Sciences, Graduate School of Convergence Science and Technology and College of Medicine or College of Pharmacy, Seoul National University, Seoul, Korea; [2]Department of Biochemistry and Biomedical Sciences, Seoul National University College of Medicine, Seoul, Korea and [3]School of Interdisciplinary Bioscience and Bioengineering & Department of Chemical Engineering, Pohang University of Science and Technology, Pohang, Korea
Correspondence: Professor EC Yi, WCU Department of Molecular Medicine and Biopharmaceutical Sciences, Graduate School of Convergence Science and Technology and College of Medicine or College of Pharmacy, Seoul National University, 28 Yeongeon-Dong, Jongno-Gu, Seoul 110-799, Korea.
E-mail: euyi@snu.ac.kr
Received 1 May 2013; accepted 7 May 2013

pentylamine tagging followed by affinity chromatography and MS analysis.[8] Despite such technical advances for *O*-GlcNAcylated protein identification and *O*-GlcNAcylation site mapping, the study of the dynamics between *O*-GlcNAcylation and phosphorylation has been limited owing to the technical difficulty of selectively co-isolating both forms. Hence, non-destructive, highly selective methods for the efficient isolation and detection of PTMs would provide valuable insights into the fundamental roles of *O*-GlcNAcylation and phosphorylation in cellular processes.

Here, we describe a method for the isolation, concurrent identification and quantification of *O*-GlcNAcylated and phosphorylated proteins. This method is based on the separation of *O*-GlcNAcylated and phosphorylated peptides using TiO_2 affinity chromatography, removal of *O*-GlcNAc and phosphate groups by β-elimination, conjugation with normal dithiothreitol (DTT; d0-DTT) or isotopically labeled DTT (d6-DTT), and isolation of DTT-conjugated peptides by thiol affinity chromatography. The isolated peptides are then identified and quantified by MS. Using this method, we investigated the concurrent transitory PTM events between *O*-GlcNAcylation and phosphorylation. Furthermore, we mapped potential reciprocal PTM sites on synapsin-1 and tau peptides isolated from mouse brain synaptosomes.

MATERIALS AND METHODS

Isolation of mouse synaptosomes

SJL mice (Jackson Labs, Bar Harbor, ME, USA) were anesthetized and killed by cervical dislocation. The hippocampus and cortex were removed and immediately stored at 4 °C in the homogenization medium (0.075 M sucrose, 0.225 M sorbitol, 1 mM ethylene glycol tetraacetic acid, 0.1% fatty acid-free bovine serum albumin and 10 mM Tris-HCl, pH 7.4). The tissue was homogenized with 10–15 strokes in a glass homogenizer. Homogenates were centrifuged to remove unbroken cells (1000 g, 5 min, 4 °C). The supernatants were collected by centrifugation at 4 °C and 12 000 *g* for 10 min. The pellet contains mitochondria and synaptosomes. The pellet was resuspended in medium B (5 mM potassium phosphate, 0.32 M sorbitol, pH 7.5) and centrifuged at 4 °C and 12 000 *g* for 10 min. The pellet was resuspended in 2 ml of medium B and then added to 14 ml of a two-phase mixture (the final concentrations of 6.4% (w/w) Dextran T500, 0.32 M sorbitol, 6.4% (w/w) polyethylene glycol, 5 mM potassium phosphate and 0.1 mM EDTA, pH 7.8). After 20 inverting of the tube, the two-phase was centrifuged at 4 °C and 1500 *g* for 1 min. At this step, the upper phase contains synaptosomes, which was added to medium A (1 mM potassium EDTA, 10 mM Tris-HCl and 0.32 M sucrose pH 7.4). Synaptosomes were obtained by centrifugation at 4 °C and 5500 *g* for 5 min.[9]

In-solution digestion of proteins

Proteins isolated from mouse brain synaptosomes were dissolved in 8 M urea and reduced with 10 mM DTT for 1 h at room temperature (RT), followed by alkylation with 30 mM iodoacetamide for 30 min at RT in the dark. Proteins were digested with sequencing grade-modified trypsin (Promega, Madison, WI, USA) at a concentration of 1:50 (w/w) overnight at 37 °C. Peptides were desalted on a C18 Sep-Pak cartridge (Waters Corp., Milford, MA, USA).

Separation of *O*-GlcNAcylated and phosphorylated peptides using a TiO_2 affinity column

A TiO_2 affinity column (GL Sciences, Torrance, CA, USA) was prewashed with 20 µl buffer A (0.5% TFA in 80% ACN) and then equilibrated with 20 µl buffer B (0.4% TFA and 25% lactic acid or acetic acid in 60% ACN). A mixture of *O*-GlcNAcylated (TAPT(***O*-GlcNAc**)STIAPG) and phosphorylated (TAPT(**phospho**)STIAPG) synthetic peptides (Invitrogen, St.Louis, MO, USA) in 150 µl buffer B was loaded onto the column. Following sample loading, the column was centrifuged at 1000 *g* for 4 min, and the flow-through fraction was saved. The column was then washed with 20 µl buffer B by centrifugation at 3000 *g* for 1 min followed by 20 µl buffer A, and the flow-through fractions were again saved. All the flow-through fractions containing *O*-GlcNAcylated peptide were combined. Phosphorylated peptide was eluted with 50 µl 5% NH_4OH by two rounds of centrifugation at 1000 *g* for 3 min, followed by centrifugation with 50 µl 30% ACN at 1000 *g* for 3 min. Both flow-through and elution fractions were desalted with a C18 Sep-Pak cartridge (Waters Corp.), which was prewashed with 100% ACN and equilibrated with 0.1% acetic acid in H_2O. The pH of the samples was adjusted to below 3.0 by adding 10% formic acid (FA), and samples were then loaded onto C18 columns. The columns were washed with 0.1% acetic acid, and the peptides were eluted with 80% ACN in 0.1% acetic acid in H_2O. Each eluate was evaporated in a Speed-Vac concentrator (Labconco, Kansas City, MO, USA). The peptides were reconstituted in Solvent A (2% ACN and 0.1% FA in H_2O) for MS analysis.

BEMAD reaction

Dried peptides were β-eliminated and subjected to BEMAD via resuspension in 90 µl 90% MeOH, 0.25 M $Ba(OH)_2$, and 10 mM d0- or d6-DTT (Cambridge Isotope Laboratories, Andover, MA, USA), and the reaction mixture was incubated at 45 °C for 2 h. The reaction was quenched by adding 0.3 M H_2SO_4 (pH 5.0). Peptides were dried, cleaned using a C18 Sep-Pak cartridge (Waters Corp.) and dried in a Speed-Vac (Labconco).

Thiol affinity chromatography

Thiopropyl sepharose 6B beads (GE HealthCare Life Sciences, Pittsburgh, PA, USA) were suspended with de-gassed high-pressure liquid chromatography (HPLC)-grade H_2O. The swelled beads were transferred onto spin columns and washed seven times with 500 µl de-gassed H_2O. Dried DTT-labeled peptides were suspended with 600 µl TBS-EDTA (20 mM Tris, 150 mM NaCl and 1 mM EDTA, pH 7.5), mixed with activated Thiopropyl sepharose beads and incubated at RT for 4 h while rotating. After incubation, beads were washed seven times with 500 µl TBS-EDTA and then incubated with elution buffer solution (20 mM free DTT in TBS-EDTA) at RT for 1 h before collecting the eluent. The elution fraction was acidified with 10% FA, desalted with a C18 Sep-Pak cartridge and dried in a Speed-Vac concentrator (Labconco). The sample was stored at −80 °C until use.

Mass spectrometry analysis

Synthetic peptides were analyzed on an Agilent 6430 triple quadrupole mass spectrometer (Agilent Technologies, Santa Clara, CA, USA) coupled with an Agilent 1200 nano-HPLC interfaced with the HPLC-chip spray system. The peptides were resuspended in solvent A (0.1% FA in water) and separated on the HPLC-chip column, ZORBAX 300SB-C18 (5 µm, 160 nl enrichment column and 75 µm × 150 mm analytical column) with a linear gradient of 0–40% solvent B (0.1% FA in ACN) for 20 min at a flow rate of 300 nl min^{-1}. The

spray voltage was set to 1.9 kV and the temperature of nitrogen drying gas was set to 325 °C in the positive ion mode. Full scan range was set from 300 to 1700 *m/z* and the scan time was set to 500 ms.

Thiol-enriched peptides were resuspended in 50 µl solvent A (2% ACN, 0.1% FA in H_2O), and 5 µl of the sample was analyzed by MS with a house-packed 75 µm (inner diameter micro-capillary) × 10-cm C_{18} column with a 2–38% gradient of solvent B (98% ACN, 0.1% FA in H_2O) for 90 min at a flow rate of 300 nl min^{-1}. MS spectra were recorded on an LTQ-velos (Thermo Fisher Scientific, San Jose, CA, USA) interfaced with a nano-HPLC system (Easy *n*LC, Thermo Fisher Scientific). Standard MS conditions were a spray voltage set to 1.9 kV and a heated capillary temperature of 325 °C. Full scans were acquired in the LTQ analyzer at 400–1400 *m/z*, and the LTQ was operated in a data-dependent mode with one survey MS scan followed by five MS/MS scans on the five most intense ions. Tandem mass spectra were analyzed using the Sorcerer-SEQUEST search engine. The search was performed using the Uniprot database for *Mus musculus* (mouse, 10090), with carbamidomethyl as a fixed modification and variable parameters set for oxidation of methionine and DTT-derivatized peptides including mass increases of 136.25 Da (d0-DTT) and 142.25 Da (d6-DTT) for serine and threonine. We also allowed for a mass increase of 120.25 Da (d0-DTT) and 126.25 Da (d6-DTT) for cysteine.

RESULTS

Metal affinity chromatographic separation of *O*-GlcNAcylated and phosphorylated peptides

We first evaluated the performance of several different metal affinity matrices (TiO_2, IMAC and ZrO_2/TiO_2) for the separation of *O*-GlcNAcylated (TAPT(***O*-GlcNAc**)STIAPG) and phosphorylated (TAPT(**phospho**)STIAPG) synthetic peptides. Peptide separation efficiency was assessed by measuring Liquid chromatography–mass spectrometry (LC-MS) peptide elution profiles. The TiO_2-column was found to provide better peptide separation efficiency than other metal affinity matrices (data not shown). Therefore, we sought to further optimize conditions for TiO_2-column separation of the retentate fraction (phosphopeptides) and the flow-through fraction (*O*-GlcNAc peptides) for the subsequent BEMAD reaction.

Figure 1 shows an LC/MS profile of the *O*-GlcNAcylated peptide (Figures 1a, M + 2H, 559.6) and the phosphorylated peptide (Figures 1b, M + 2H, 498.2) isolated from the TiO_2-column separation with a lactic acid sample loading/binding buffer. The peak area of extracted ion chromatogram of the *O*-GlcNAcylated peptide was much less than the level of the phosphorylated peptide. Moreover, the LC/MS profile of the *O*-GlcNAcylated peptide fraction showed multiple peaks eluted at the late chromatographic gradient condition, indicating that the C18 sample clean-up did not completely remove the acid and other unknown impurities. We also found that owing to its high viscosity and acidity, the lactic acid present in the column-binding buffer interfered with the BEMAD reaction for the flow-through fraction (containing the *O*-GlcNAcylated peptide). Replacing lactic acid with acetic acid in the sample loading/binding buffer improved the *O*-GlcNAcylated peptide recovery (Figure 2).

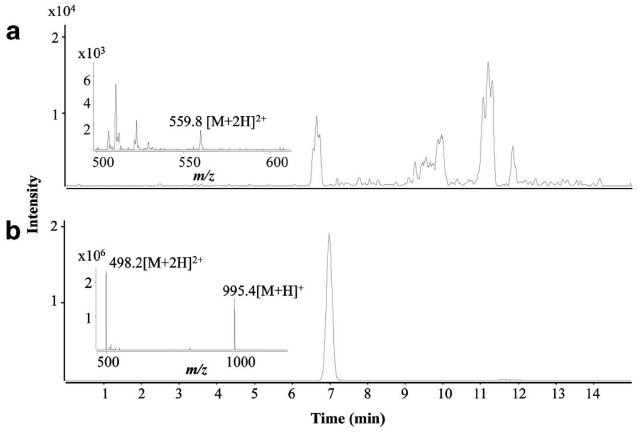

Figure 1 Separation of synthetic peptides using TiO_2 affinity chromatography with a lactic acid sample loading/binding buffer. (**a**) Extracted ion chromatogram of the TiO_2-column flow-through fraction, with the inset showing the doubly charged peptide ion (*m/z*, 559.8) corresponding to the *O*-GlcNAcylated synthetic peptide (TAPT(***O*-GlcNAc**)STIAPG). (**b**) Extracted ion chromatogram of the TiO_2-column retentate fraction, with the inset showing singly (*m/z*, 995.4) and doubly (*m/z*, 498.2) charged peptide ions corresponding to the phosphorylated synthetic peptides (TAPT(**phospho**)STIAPG).

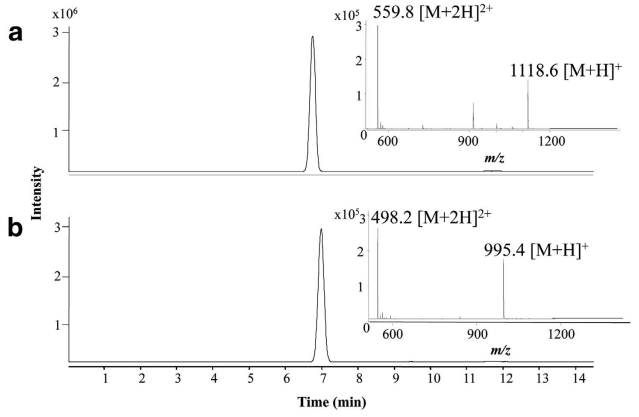

Figure 2 Separation of synthetic peptides using TiO_2 affinity chromatography with an acetic acid-binding buffer. (**a**) Extracted ion chromatogram of the TiO_2-column flow-through fraction, with the inset showing singly (*m/z*, 1118.6) and doubly (*m/z*, 559.8) charged peptide ions corresponding to the *O*-GlcNAcylated synthetic peptide (TAPT(***O*-GlcNAc**)STIAPG). (**b**) Extracted ion chromatogram of the TiO_2-column elution fraction, with the inset showing singly (*m/z*, 995.4) and doubly (*m/z*, 498.2) charged peptide ions corresponding to the phosphorylated peptides (TAPT(**phospho**)STIAPG). The ratio between the two peptides was 1:1.

Selective enrichment of *O*-GlcNAcylated and phosphorylated synthetic peptides in a complex peptide mixture

With the acetic acid modifier, we further evaluated the TiO_2-column for selective isolation of *O*-GlcNAcylated and phosphorylated synthetic peptides in a complex peptide sample mixture. Equal amounts of *O*-GlcNAcylated and

phosphorylated synthetic peptides (1 pmol each) were mixed with 400 μg trypsin-digested peptides obtained from mouse brain synaptosomal proteins. After separation of the peptide mixtures using the TiO_2-column, the retentate and flow-through fractions were analyzed by selected ion monitoring for both the *O*-GlcNAcylated (M + 2H, 559.6) and phosphorylated (M + 2H, 498.2) peptides using a triple quadruple mass spectrometer. We detected only the phosphorylated peptide (Figure 3b) but not the *O*-GlcNAcylated peptide (Figure 3a). However, when the flow-through and retentate fractions were processed with the BEMAD reaction, labeled with d0-DTT and d6-DTT, and purified using thiol affinity chromatography, we detected both d0-DTT-labeled phosphorylated peptide (Figure 4a) and d6-DTT-labeled *O*-GlcNAcylated peptide (Figure 4b). Their corresponding ions (peptide masses), phosphorylated peptide (M + H, 1051.4) and *O*-GlcNAcylated peptide (M + H, 1057.4) (Figure 4c) were detected with an equal intensity (expected ratio of 1:1) with a mass difference of 6 Da. These results indicate that the *O*-GlcNAcylated and phosphorylated peptides present in the complex mixture were well separated and selectively enriched through the TiO_2-column separation and thiol affinity chromatography.

Concurrent identification and quantification of *O*-GlcNAcylated and phosphorylated sites of synapsin-1 and tau proteins in mouse brain synaptosomes

Next, we attempted to identify *O*-GlcNAcylated and phosphorylated site modifications of cytoplasmic and nuclear proteins in mouse brain synaptosomes. The isolated proteins were trypsinized, and the resulting tryptic peptides were separated into phosphorylated and *O*-GlcNAcylated fractions using the TiO_2-column and labeled with d0-DTT and d6-DTT, respectively (Figure 5). Mixed d0/d6-DTT-labeled peptides were enriched with thiol affinity chromatography and then analyzed by liquid chromatography–mass spectrometry. By searching a sequence database, we identified peptide sequences of both synapsin-1 and tau showing potential reciprocal sites between *O*-GlcNAcylation and phosphorylation. andem MS spectra of the synapsin-1 peptide sequence

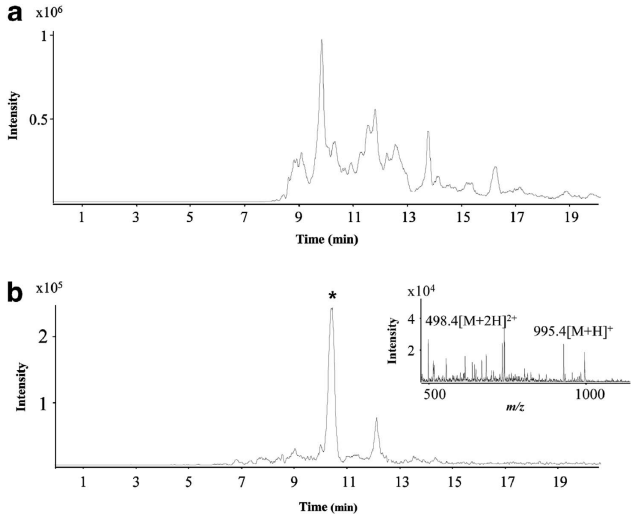

Figure 3 Detection of *O*-GlcNAcylated and phosphorylated peptides in a complex peptide mixture (synaptosome) via TiO_2 affinity enrichment using an acetic acid-binding buffer. (**a**) LC/MS trace of the TiO_2-column flow-through fraction of *O*-GlcNAcylated and phosphorylated peptides (1:1 ratio) in a complex peptide mixture. (**b**) LC/MS trace of the TiO_2-column retentate fraction of *O*-GlcNAcylated and phosphorylated peptides (1:1 ratio) in a complex peptide mixture. Extracted ion chromatogram of the phosphorylated peptide (marked with an asterisk), with the inset showing singly (*m*/*z*, 995.4) and doubly (*m*/*z*, 498.2) charged peptide ions corresponding to the phosphorylated peptides (TAPT **(phospho)**STIAPG).

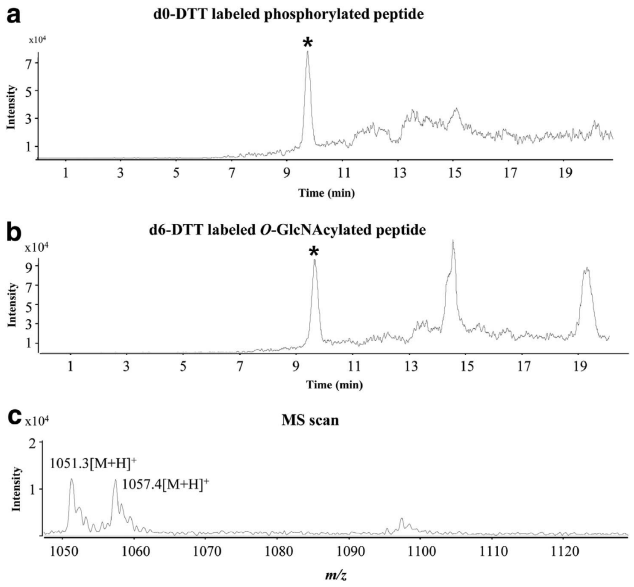

Figure 4 Selective enrichment of *O*-GlcNAcylated and phosphorylated synthetic peptides in a synaptosome sample via BEMAD followed by thiol affinity chromatography. (**a**) LC/MS trace of d0-DTT-conjugated phosphorylated peptide. (**b**) LC/MS trace of d6-DTT-conjugated *O*-GlcNAcylated peptide. (**c**) MS trace of singly charged d0-DTT-labeled phosphorylated peptide (M + H, 1051.4) and d6-DTT-labeled *O*-GlcNAcylated peptide (M + H, 1057.4).

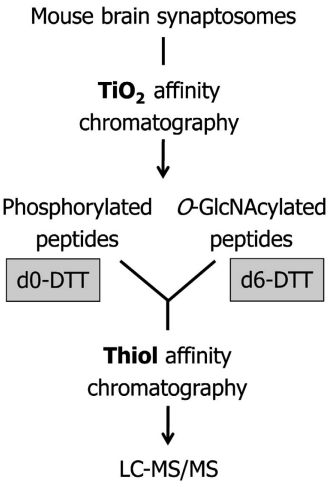

Figure 5 Experimental workflow for concurrent identification of phosphorylated and *O*-GlcNAcylated peptides.

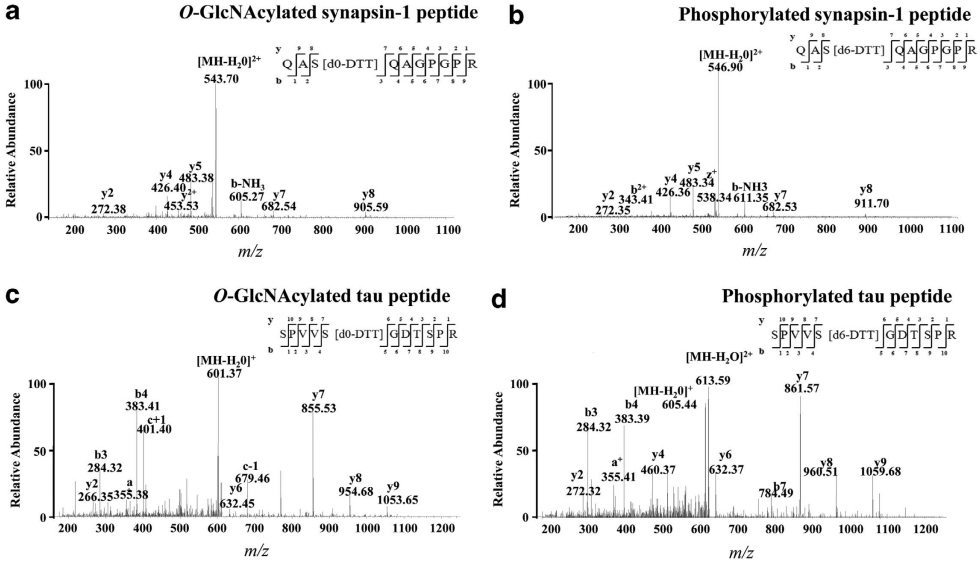

Figure 6 Tandem spectra of d0-DTT- and d6-DTT-labeling of synaptin-1 and tau peptides. (**a**) Tandem spectrum of d0-DTT- and (**b**) d6-DTT-labeling at the Ser^{605} residue of the synapsin-1 peptide ^{603}QASQAGPGPR^{612}. (**c**) Tandem spectrum of d0-DTT- and (**d**) d6-DTT-labeling at the Ser^{692} residue of the tau peptide ^{688}SPVVSGDTSPR^{698}. All corresponding a-, b- and y-ion series are assigned.

^{603}QASQAGPGPR^{612} showed that the Ser^{605} residue was conjugated with either d0-DTT (Figure 6a) or d6-DTT (Figure 6b), indicating that this residue was formerly modified by either phosphorylation or *O*-GlcNAcylation, respectively. We also identified the Ser^{692} residue of a tau peptide ^{688}SPVVSGDTSPR^{698}, and its tandem MS spectra clearly indicated that this residue was modified by either *O*-GlcNAcylation (Figure 6c) or phosphorylation (Figure 6d). These results were further confirmed by an *O*-GlcNAcylation prediction tool (dbOGAP, http://cbsb.lombardi.georgetown.edu/OGAP.html)[10] and a phosphorylation prediction tool (NetPhos 2.0 server, http://www.cbs.dtu.dk/services/NetPhos).[11] The Ser^{605} residue of synapsin-1 was predicted to be a site of both phosphorylation (prediction score, 0.933) (Figure 7a) and *O*-GlcNAcylation (prediction score, 0.4188) (Figure 7b), and it also appeared to be a potential reciprocal site (Figure 7c) based on the results of another prediction tool (YinOYang 1.2, http://www.cbs.dtu.dk/services/YinOYang).[12] Using the same prediction tools, the Ser^{692} residue of the tau peptide ^{688}SPVVSGDTSPR^{698} was also predicted to be a site of phosphorylation (prediction score, 0.792) (Figure 7d) and *O*-GlcNAcylation (prediction score, 0.6152) (Figure 7e), as well as a potential reciprocal site (Figure 7f).

DISCUSSION

Recent advances in techniques for enriching *O*-GlcNAcylated and phosphorylated peptides followed by identification of either site modification on ser/threonine residues by MS analysis have facilitated studies of the fundamental roles of protein *O*-GlcNAcylation in cellular processes. Despite the importance of the reciprocal relationship between protein *O*-GlcNAcylation and phosphorylation in nuclear transport, transcription and translation, signal transduction, cytoskeletal reorganization, proteasomal degradation and apoptosis,[3] a reliable method for concurrently identifying *O*-GlcNAcylation and phosphorylation is needed to enhance our knowledge of key regulatory post-translational dynamics in cellular processes. This report describes our strategy for concurrently identifying *O*-GlcNAcylated and phosphorylated peptides in a quantitative manner using TiO_2-column enrichment and BEMAD methods. Although this strategy is similar to that used to identify *O*-GlcNAcylated proteins,[8] we implemented combined metal affinity chromatography and BEMAD approaches to concurrently enrich *O*-GlcNAcylated and phosphorylated peptides and thereby map the two PTMs at the same time.

Metal affinity chromatography utilizing TiO_2, IMAC or ZnO_2 enriches phosphorylated peptides through chelating phosphate groups at the immobilized divalent cation. As a result, peptide mixtures can be separated into column retentate and flow-through fractions, with the retentate fraction mostly containing phosphorylated peptides and the flow-through fraction mostly containing *O*-GlcNAcylated peptides and other non-phosphorylated peptides. Out of the three different types of metal affinity chromatographic columns, we found that TiO_2-based column chromatography affords the most efficient separation between phosphorylated and *O*-GlcNAcylated peptides. As lactic acid in the TiO_2-based column chromatography interfered with the DTT conjugation reaction onto the peptides, we replaced the acid modifier with acetic acid. A major benefit of using acetic acid for peptide separation is that the acid can be easily removed from the flow-through fraction by simple vacuum evaporation. We also found that DTT conjugation to the peptide mixtures in the flow-through fraction reduced the sample complexity by isolating a subset of peptides, thereby enhancing *O*-GlcNAcylated peptide detection. As the BEMAD reaction also affects cysteine-containing peptides in the flow-through fraction, however, perchlorate

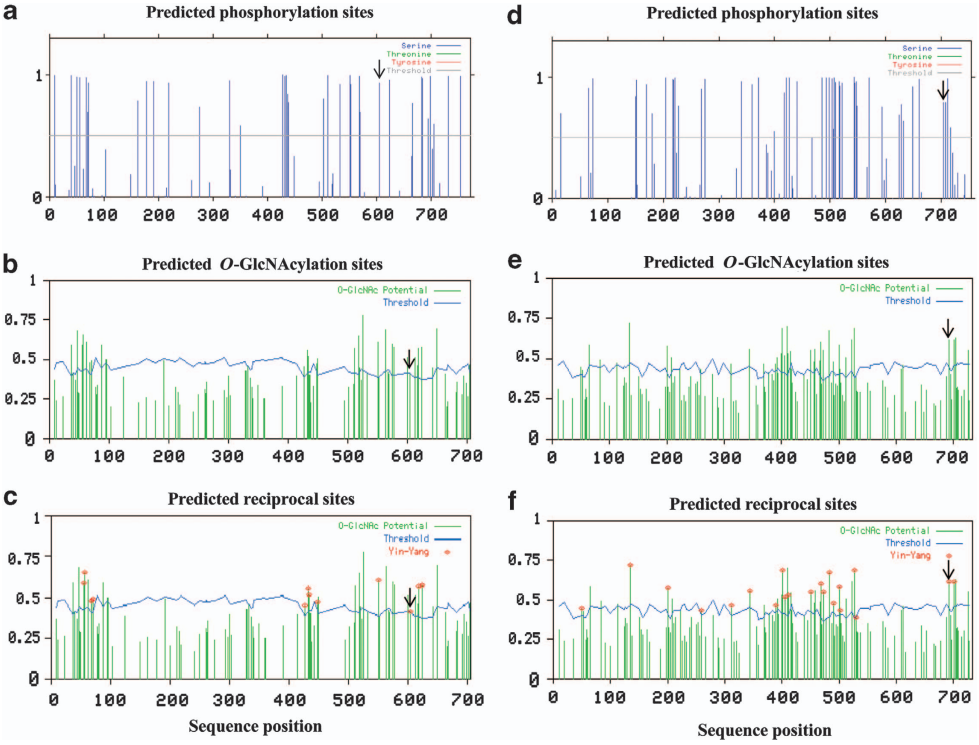

Figure 7 Prediction of phosphorylation, *O*-GlcNAcylation and reciprocal sites for synapsin-1 and tau. (**a**) Predicted phosphorylation sites and (**b**) *O*-GlcNAcylation sites of synapsin-1. Prediction scores of phosphorylation and *O*-GlcNAcylation for Ser^{605} (marked by an arrow) were >0.5, and (**c**) the serine residue was identified as a potential reciprocal site (Ying–Yang score of 0.5). The horizontal line indicates the threshold (0.5) for modification potential, and the vertical lines show the potential phosphorylation and *O*-GlcNAcylation sites for the serine residue in the synapsin-1 peptide. (**d**) Predicted phosphorylation sites and (**e**) *O*-GlcNAcylation sites of tau. Prediction scores of phosphorylation and *O*-GlcNAcylation for Ser^{692} (marked by an arrow) were greater than 0.7 and (**f**) the serine residue as identified as a potential reciprocal site (Ying–Yang score of 0.6).

oxidation of the cysteine residues may reduce the co-purification of cysteine-containing peptides with *O*-GlcNAcylated peptides.[8] Nonetheless, we successfully demonstrated that the TiO_2-column enrichment/BEMAD reaction enables the reciprocal site mapping of synapsin-1 and tau proteins in mouse brain synaptosomes. By mapping *O*-GlcNAcylated and phosphorylated sites on synaptin-1, we identified that Ser^{605} in the synapsin-1 peptide sequence ^{603}QASQAGPGPR^{612} is both phosphorylated and *O*-GlcNAcylated. These findings are consistent with previous studies in which *O*-GlcNAcylation of a specific serine residue was found to modulate its regulatory function.[13] Several research groups, including that of Jovanovic *et al.*, report that this neuronal protein regulates synaptic vesicle trafficking through a reciprocal process between phosphorylation and dephosphorylation of specific synapsin-1 sites,[14–16] and this particular serine residue is reported to be a potential reciprocal site involved in regulating hippocampal synaptic plasticity.[17] We also identified that Ser^{692} in the tau peptide sequence ^{688}SPVVSGDTSPR^{698} is a potential reciprocal site in mouse brain synaptosomes. Interestingly, concurrent alterations of tau *O*-GlcNAcylation and phosphorylation have been found to be involved in impaired brain glucose uptake/metabolism.[18]

In conclusion, we demonstrated that a combined TiO2 affinity separation and BEMAD method allows selective enrichment of *O*-GlcNAcylated and phosphorylated peptides, which permits the assessment of potential cross-talk between these two PTMs and their regulatory roles. To the best of our knowledge, this is the first systematic assessment of specific serine reciprocal site occupancy of *O*-GlcNAcylation and phosphorylation of synapsin-1 and tau in mouse brain synaptosomes. Future studies can provide further validation of their functional roles in the pathogenesis of various human diseases such as diabetes, Alzheimer's disease and cancer.

CONFLICT OF INTEREST

The authors declare no conflict of interest.

ACKNOWLEDGEMENTS

This research was supported by grant No. R31-2008-000-10103-0 from the World Class University program of the Ministry of Education, Science, and Technology, and the National Research Foundation of Korea, and the Proteogenomic Research Program through the National Research Foundation of Korea.

Author contributions: The manuscript was written through contributions of all authors. All authors have given approval to the final version of the manuscript.

1 Laczy B, Hill BG, Wang K, Paterson AJ, White CR, Xing D *et al*. Protein O-GlcNAcylation: a new signaling paradigm for the cardiovascular system. *Am J Physiol Heart Circ Physiol* 2009; **296:** H13–H28.
2 Hart GW, Housley MP, Slawson C. Cycling of O-linked β-N-acetylglucosamine on nucleocytoplasmic proteins. *Nature* 2007; **446:** 1017–1022.
3 Hart GW, Slawson C, Ramirez-Correa G, Lagerlof O. Cross talk between O-GlcNAcylation and phosphorylation: roles in signaling, transcription, and chronic disease. *Ann Rev Biochem* 2011; **80:** 825.
4 Mishra S, Ande S, Salter N. O-GlcNAc modification: why so intimately associated with phosphorylation? *Cell Commun Signal* 2011; **9:** 1.
5 Vosseller K, Trinidad JC, Chalkley RJ, Specht CG, Thalhammer A, Lynn AJ *et al*. O-linked N-acetylglucosamine proteomics of postsynaptic density preparations using lectin weak affinity chromatography and mass spectrometry. *Mol Cell Proteomics* 2006; **5:** 923–934.
6 Trinidad JC, Barkan DT, Gulledge BF, Thalhammer A, Sali A, Schoepfer R *et al*. Global identification and characterization of both O-GlcNAcylation and phosphorylation at the murine synapse. *Mol Cell Proteomics* 2012; **11:** 215–229.
7 Wang Z, Pandey A, Hart GW. Dynamic interplay between O-linked N-acetylglucosaminylation and glycogen synthase kinase-3-dependent phosphorylation. *Mol Cell Proteomics* 2007; **6:** 1365–1379.
8 Wells L, Vosseller K, Cole RN, Cronshaw JM, Matunis MJ, Hart GW. Mapping sites of O-GlcNAc modification using affinity tags for serine and threonine post-translational modifications. *Mol Cell Proteomics* 2002; **1:** 791–804.
9 Fernández-Vizarra E, López-Pérez MJ, Enriquez JA. Isolation of biogenetically competent mitochondria from mammalian tissues and cultured cells. *Methods* 2002; **26:** 292–297.
10 Wang J, Torii M, Liu H, Hart GW, Hu Z-Z. dbOGAP-an integrated bioinformatics resource for protein O-GlcNAcylation. *BMC Bioinform* 2011; **12:** 91.
11 Blom N, Gammeltoft S, Brunak S. Sequence and structure-based prediction of eukaryotic protein phosphorylation sites. *J Mol Biol* 1999; **294:** 1351.
12 Gupta R, Brunak S. Prediction of glycosylation across the human proteome and the correlation to protein function. *Pac Symp Biocomput* 2002; **7:** 310–322.
13 Christie G, Markwell RE, Gray CW, Smith L, Godfrey F, Mansfield F *et al*. Alzheimer's disease. *J Neurochem* 1999; **73:** 195–204.
14 Jovanovic JN, Sihra TS, Nairn AC, Hemmings HC, Greengard P, Czernik AJ. Opposing changes in phosphorylation of specific sites in synapsin I during Ca2+-dependent glutamate release in isolated nerve terminals. *J Neurosci* 2001; **21:** 7944–7953.
15 Liu F, Iqbal K, Grundke-Iqbal I, Hart GW, Gong C-X. O-GlcNAcylation regulates phosphorylation of tau: a mechanism involved in Alzheimer's disease. *Proc Natl Acad Sci USA* 2004; **101:** 10804–10809.
16 Deng Y, Li B, Liu F, Iqbal K, Grundke-Iqbal I, Brandt R *et al*. Regulation between O-GlcNAcylation and phosphorylation of neurofilament-M and their dysregulation in Alzheimer disease. *FASEB J* 2008; **22:** 138–145.
17 Tallent MK, Varghis N, Skorobogatko Y, Hernandez-Cuebas L, Whelan K, Vocadlo DJ *et al*. *In vivo* modulation of O-GlcNAc levels regulates hippocampal synaptic plasticity through interplay with phosphorylation. *J Biol Chem* 2009; **284:** 174–181.
18 Li X, Lu F, Wang JZ, Gong CX. Concurrent alterations of O-GlcNAcylation and phosphorylation of tau in mouse brains during fasting. *Eur J Neurosci* 2006; **23:** 2078–2086.